

Shan Jiang,
Genyang Cao,
Guangming Cai,
Weilin Xu,
Wenbin Li,
Xin Wang¹

School of Textile Science and Engineering,
Wuhan Textile University,
Wuhan 430200, China

¹School of Fashion and Textiles,
RMIT University,
Melbourne 3056, Australia
E-mail: xin.wang@rmit.edu.au

Unidirectional Torsion Properties of Single Silk Fibre

DOI: 10.5604/12303666.1196608

Abstract

The unidirectional torsion properties of silk fibre were investigated on a purpose-built single fibre torsion tester. The torsional fracture angle and the number of cycles of torsion at breaking were recorded, and the effect of the gauge length and pretension together with the torsion speed on the torsion properties of single silk fibre was investigated in detail. Scanning electron microscopy (SEM), X-ray diffraction (XRD) analysis and a tensile tester were used to understand the morphology, structure and tensile properties of silk fibre after torsion deformation. SEM photos show that silk fibre exhibits a ribbon-like profile after torsion, and fracture tends to occur at both ends of the silk fibre, where a larger number of twists can be observed. The crystallinity calculated from XRD spectra of silk fibre increases from 26.11% to 34.10% after torsion. The breaking stress and strain decreases slightly with an increase in the gauge length. The breaking cycle increases linearly with an increase in the gauge length, while the actual torsional fracture angle decreases gradually at the same time. The torsional fracture angle together with the breaking cycle decreases gradually as the pretension increases. The fracture angle together with the breaking cycle increases with an increase in the torsion speed. Understanding the unidirectional torsion properties of single silk fibre will benefit its further application in specific areas where the fibre will be subject to frequent torsion and deformation.

Key words: unidirectional torsion, silk fibre, fracture angle, breaking cycle, SEM, XRD.

Introduction

Mulberry silk fibre exhibits excellent mechanical properties, such as high tenacity, high elongation and strong energy absorption capacity. It is widely used in textiles, tissue engineering and biomedical materials and composites [1]. Intensive study has been conducted to understand the unique mechanical properties of silk fibre. Related research work has focused on the effect of the harvesting conditions on the mechanical properties of *B. mori* silk [2], the mechanical properties of silkworm silk under different conditions [3], the relationship between the mechanical properties and structure of silk [4, 5], and changes in the mechanical properties and structures of *B. mori* silk exposed to biodegradation [6]. Despite the fact that mechanical properties determine the performance and lifetime of composites, research work mainly focuses on the tensile properties of silk fibre in composites. Composites are subject to different kinds of deformation in use, such as elongation, compression and torsional deformation. The torsional response of silk determines not only the final mechanical properties of as-produced composites, but also indicates their durability. Even though the torsional behaviour of silk is different when it is inside and outside of a matrix of composites, the torsional behaviour of single silk benefits the understanding of its properties within composites. Furthermore silk fibre is usually

blend spun into textile products for application due to its poor spinnability. In this process, silk fibre is subject to torsional deformation, which affects the spinning process and quality of the final products. It is thus necessary to investigate the torsional properties of silk fibre.

The torsional properties of fibres have been investigated to some extent, with researchers mainly focusing on the torsional fatigue of fibres. An investigation on the torsional fatigue performance of polyethylene and polyester found that the torsional strain amplitude had a great influence on the fatigue life of the fibre, and the breaks under different conditions were quite unlike each other [7]. Xu [8] studied the repeated torsional fatigue of wool fibre and commonly used synthetic fibres, and found that the synthetic fibres were superior to wool ones in resistance to torsion fatigue, and fibres with poor torsion fatigue resistance were not easy to pill. Liu [9] tested the torsional fatigue properties of para aramid fibre and found that there was a liner relationship between the pretension, torsional angle and natural logarithm of the fatigue life. Feng [10] studied the torsional fatigue of several high performance fibres and found that different fibres showed different fracture morphology after torsion, with most samples tending to break in the drive end. However, research work has not provided a systematic understanding of the effect of various influential factors on the torsion performance due to the lack

of a sophisticated instrument, and mainly focused on the torsional fatigue of fibres. Actually the unidirectional torsion fatigue reflects the properties of fibre in withstanding repeated torsion or deformation, and thus should be investigated thoroughly.

In this study, purpose built apparatus from a single fibre torsion tester was applied to test the unidirectional torsion properties of silk fibre. Experimental parameters such as pretension, torsion speed and gauge length were investigated in detail. The fracture morphology from scanning electron microscopy and the crystalline structure from X-ray diffraction and the tensile strength were also tested to understand the structure-property mechanism of silk fibre in torsional deformation.

Experimental

Materials

Silkworm eggs (Qiufengbaiyu, Zhejiang, China) were purchased from a market. Silkworm cocoons (average weight 0.33 g) were obtained after the process of hatching, larva and pupa. Silk fibre was subsequently taken from the silkworm cocoons.

Characterisations

Tensile tests were performed on a universal single fibre tester (Favimat+Robot2

and Airobot2, Textechno Textile Testing Technology, Germany). The retention was set as 0.5 cN/tex and the drawing speed - 20.0 mm/min. The gauge length was set as 5, 10, 15, 20 and 25 mm. 50 tests were conducted for one sample and the results averaged.

The surface morphology and fracture of the silk fibre were observed on a scanning electron microscope (JSM-6510LV, JEOL, USA). The sample was coated with gold and the accelerating voltage was set as 10 kV.

X-ray diffraction spectra were obtained from a D8 advance X-ray Diffractometer (Bruker Corporation, Germany) with monochromatic Cu K α radiation. The measurements were carried out at 40 kV and 40 mA, with a detector placed on a goniometer scanning a range from 5 to 70°, at a scan speed of 10 °/min. JADE software was used to calculate the crystallinity from the XRD spectra according to the following equation:

$$C = \frac{Ac}{Ac + Aa} \times 100 \text{ in \%} \quad (1)$$

where, C is the crystallinity, Ac the area of the crystalline peak, and Aa is the area of the amorphous peak.

Unidirectional torsion failure tests

Purpose-built apparatus was built to test the torsion performance of single silk fibre, as shown in **Figure 1.a**. It is composed of a motor driven chuck clamp 2 and U shaped holder 3, forming a gauge in the test. A testing sample was prepared by sandwiching a single fibre into hard papers using hot melt adhesive, and then the sample was placed in between the U shaped holder 4 with the other end of the fibre clamped by the chuck clamp 2. The chuck clamp 2 rotated at a specific speed during the test, while the lower end of the fibre was stabilised by the U shaped holder so that torsion was exerted on the fibre tested. A Γ -shaped shelf and sensor are placed together on the lifting table, the height of which can be adjusted through the screw lifting support. The rotation of the motor was controlled by a computer so that the cycle of rotation was recorded at the breaking of the fibre (on-off controlled by the sensor).

The gauge length can be adjusted between 5 - 25 mm by screwing the lifting table 6. Pretension was exerted on the single fibre by the hard paper of the sample,

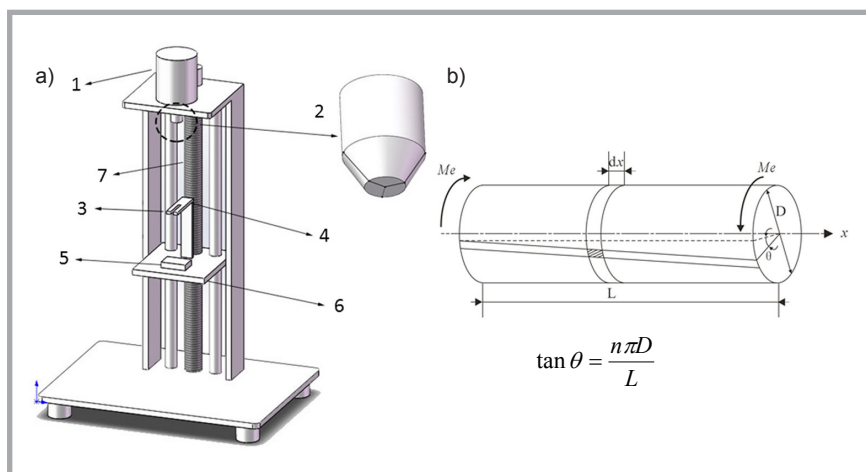


Figure 1. a) Structure of torsion tester; 1 - motor; 2 - chuck clamp, 3 - U-shaped hole, 4 - Γ -shaped shelf, 5 - sensor, 6 - lifting table, 7 - screw lifting support, b) Schematic diagram of unidirectional torsion deformation.

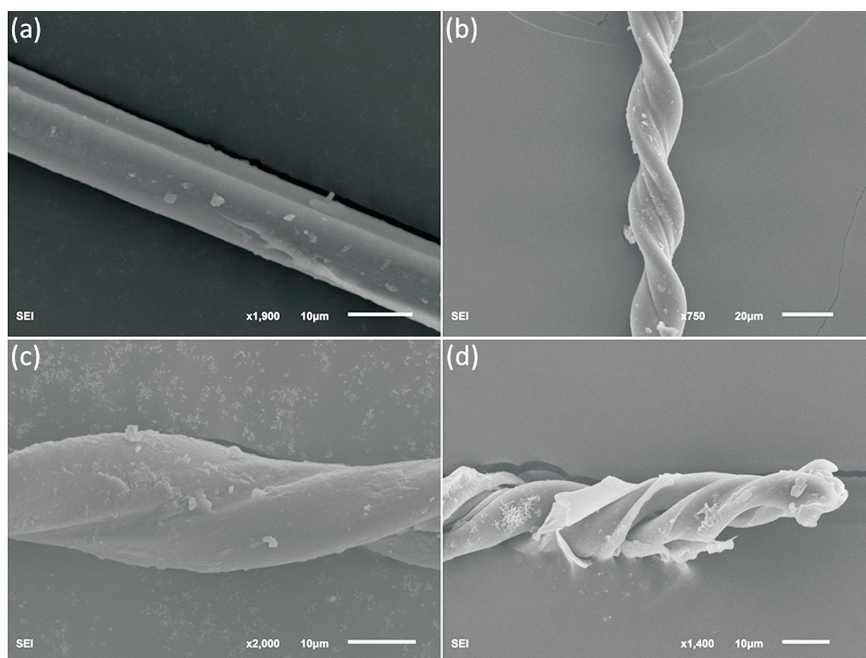


Figure 2. SEM images of original silk fibre and fibres after torsion: a) original sample, b) sample after torsion, c) magnified view of sample after torsion, d) end morphology after torsion fracture.

the weight of which can be adjusted to set a pretension from 10 to 60% of the tenacity of the fibre. The motor speed, namely the torsion speed, can be tuned to between 250 - 2000 r.p.m. For a conventional test, a gauge length of 10 mm, a pretension of 20% of the tenacity and a torsion speed of 1000 r.p.m. were selected. However, the gauge length, pretension and torsion speed were changed so as to investigate their effects on the torsion properties of the sample.

Figure 1.b shows the schematics of unidirectional torsion deformation. The torsion angle θ can be calculated according to the equation:

$$\tan \theta = \frac{n\pi D}{L} \quad (2)$$

where, n is the number of laps of the unidirectional torsion fracture, D the diameter of the fibre, and L is the gauge length.

Results and discussion

Morphology

Figure 2 shows the morphology of silk fibre before and after torsion. **Figure 2.a** illustrates the profile of silk fibre, which consists of two parallel fibroin filaments that are stuck together by sericin. **Figure 1.b** shows the morphology of silk fibre after torsion. Obvious spirals can

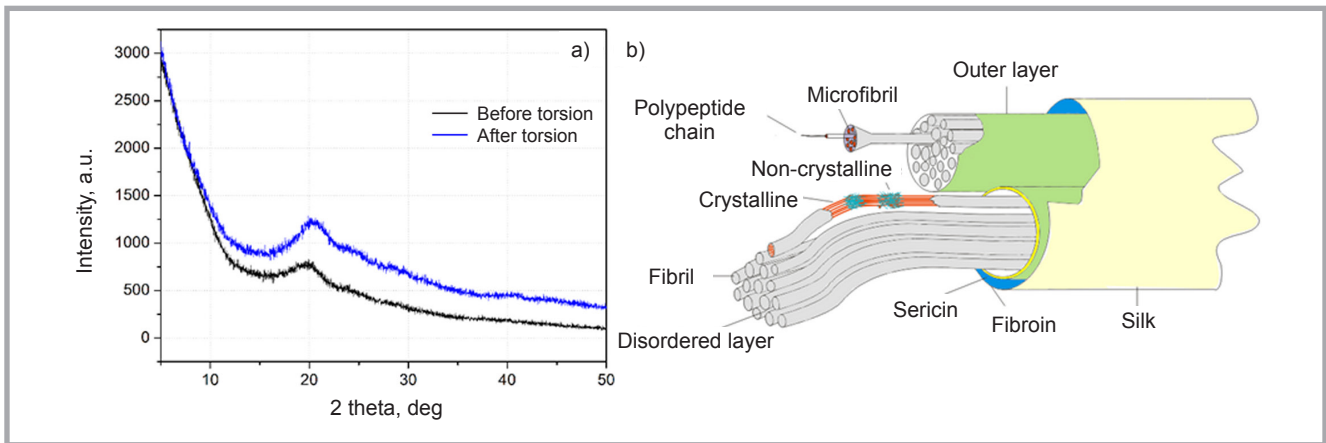


Figure 3. (a) X-ray diffraction spectra for silk fibre before and after torsion, (b) schematics of the structure of silk fibre.

be found on the surface of the fibre due to the twisting from torsion. The detailed view in **Figure 2.c** shows a ribbon-like profile of silk fibre after torsion, in which the two fibroin filaments are located side by side to form a helix. It is evident that sericin protects the two fibroin filaments after torsion, thus the deformation of the filaments occurs concurrently. **Figure 2.d** shows a typical fracture of one end of silk fibre, which can be regarded as an accumulation of plastic deformation. In the torsion process, twist occurs at both ends of the silk and then transfers longitudinally to the middle part. Fracturing tends to occur at both ends of the silk, where larger number of twists can be observed, as shown in **Figure 2.d**. It is evident that silk products will probably break from the end parts of the fibre, and the fibre will exhibit a ribbon figure in torsional deformation.

XRD analysis

Preliminary investigation using Fourier Transform Infrared Spectroscopy (FTIR)

analysis of silk fibre before and after torsion showed no observable changes in the spectra, indicating intact chemical components of silk fibre after torsion.

Figure 3.a shows the X-ray diffraction spectra for silk fibres before and after torsion. Both curves show one main peak at 20.63°, indicating the characteristic peak of a β-sheet crystalline structure. The peak at 20.63° after torsion becomes more evident, as shown in **Figure 3.a**. No other obvious changes can be observed from the curves, suggesting that torsion does not bring evident destruction to the crystalline structure of silk fibre.

The crystallinity of silk fibre calculated changes from 26.11% to 34.10% after torsion. The increased crystallinity is due to the newly formed crystalline structure after torsion. The fibril of fibroin consists of crystalline and amorphous regions, as shown in **Figure 3.b** with a structure diagram of silk fibre. It is estimated that uni-

directional torsion is not strong enough to pull polypeptide chains out from the crystalline area. However, the macromolecular chains in the non-crystalline area are stretched due to the torsion deformation. Polypeptide chains in the amorphous area are thus closer and well aligned to each other, and the cohesive force between them is strengthened by the torsional force. These changes have transferred part of the amorphous region into the crystalline region to some extent, thus the overall crystallinity increases after torsion.

Tensile properties of single silk fibre

The mechanical properties of silk fibre under different gauge lengths were tested to determine the pretension for a further unidirectional torsion test. **Figure 4** shows the tenacity and elongation at break for silk fibre under different gauge lengths. Both the mean value of the stress and strain decreases slightly with an increase in the gauge length, even though the high standard deviation makes the trend unapparent. The probability of the emergence of weak points increases at a long gauge length, hence the elongation decreases and so does the breaking stress.

Effect of the gauge length on unidirectional torsion performance

Assuming that the diameter of fibre and the torsional fracture angle are constant, **Equation 2** can be transformed into the following:

$$\frac{\tan \theta}{\pi D} = \frac{n}{L} \tag{3}$$

It suggests that the breaking cycle *n* is proportional to the gauge length.

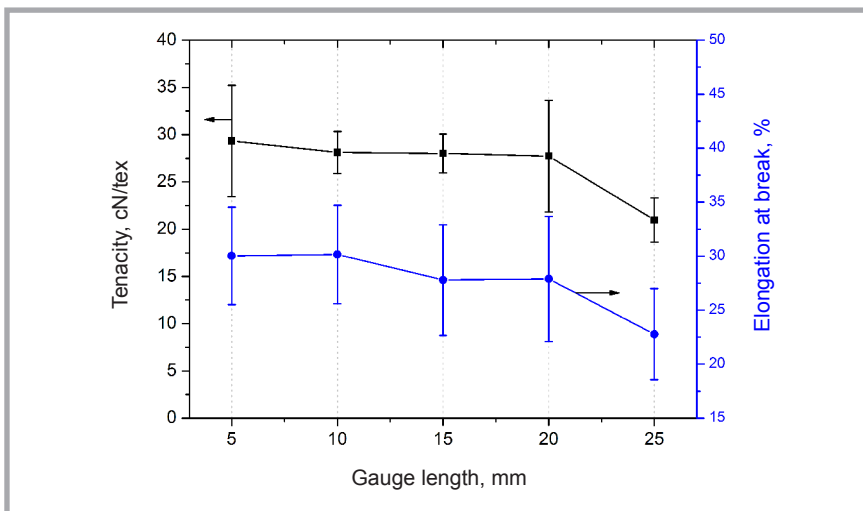


Figure 4. Influence of the gauge length on the tenacity.

Figure 5.a shows the torsional fracture angle and breaking cycle under different gauge lengths in the torsional test. It can be seen that the breaking cycle increases linearly with an increase in the gauge length, fitting quite well with **Equation 3**. The slope of the fitting line can be obtained from equation (3) as follows:

$$\text{Slope} = \frac{\tan \theta}{\pi D} \quad (4)$$

The torsional fracture angle θ has been calculated accordingly, and the value is 49° .

The torsional fracture angle tested from **Figure 5.a** fluctuates between 45° to 60° with the increasing gauge length. The mean value is 51.54 ± 3.00 , which is close to 49° . It is noted that with an increase in the gauge length from 5 to 20 mm, the torsional fracture angle decreases gradually. This is because the possibility of the emerging of a weak point is higher when the gauge length increases; therefore, the longer the fibre, the smaller the torsional fracture angle. The data of the breaking cycle under a gauge length of 25 mm is much higher than the value on the fitting line, thus a relatively higher fracture angle appears.

Effect of pretension on the unidirectional torsion performance

Pretension has an evident influence on the torsion performance, as shown in **Figure 5.b**. The torsional fracture angle together with the breaking cycle decreases gradually as the pretension increases from 10 to 50% of the tenacity. Too high a pretension, such as 60% of the tenacity, will lead to a drop in the fracture angle and breaking cycle. The main reason is that the fibre is subjected to drawing and shearing during the torsion process. With an increase in the pretension, silk fibre undergoes from shearing dominant deformation to drawing dominant deformation. The drawing effect would definitely contribute to the fracture of fibre, which finally leads to a decrease in the fracture angle and breaking cycle. It is obvious that silk fibre shows poor torsional properties when it is subjected to high pretension. Proper pretension in the spinning process will thus optimise the properties of spun yarn and products. And silk composites would endure moderate tension during usage.

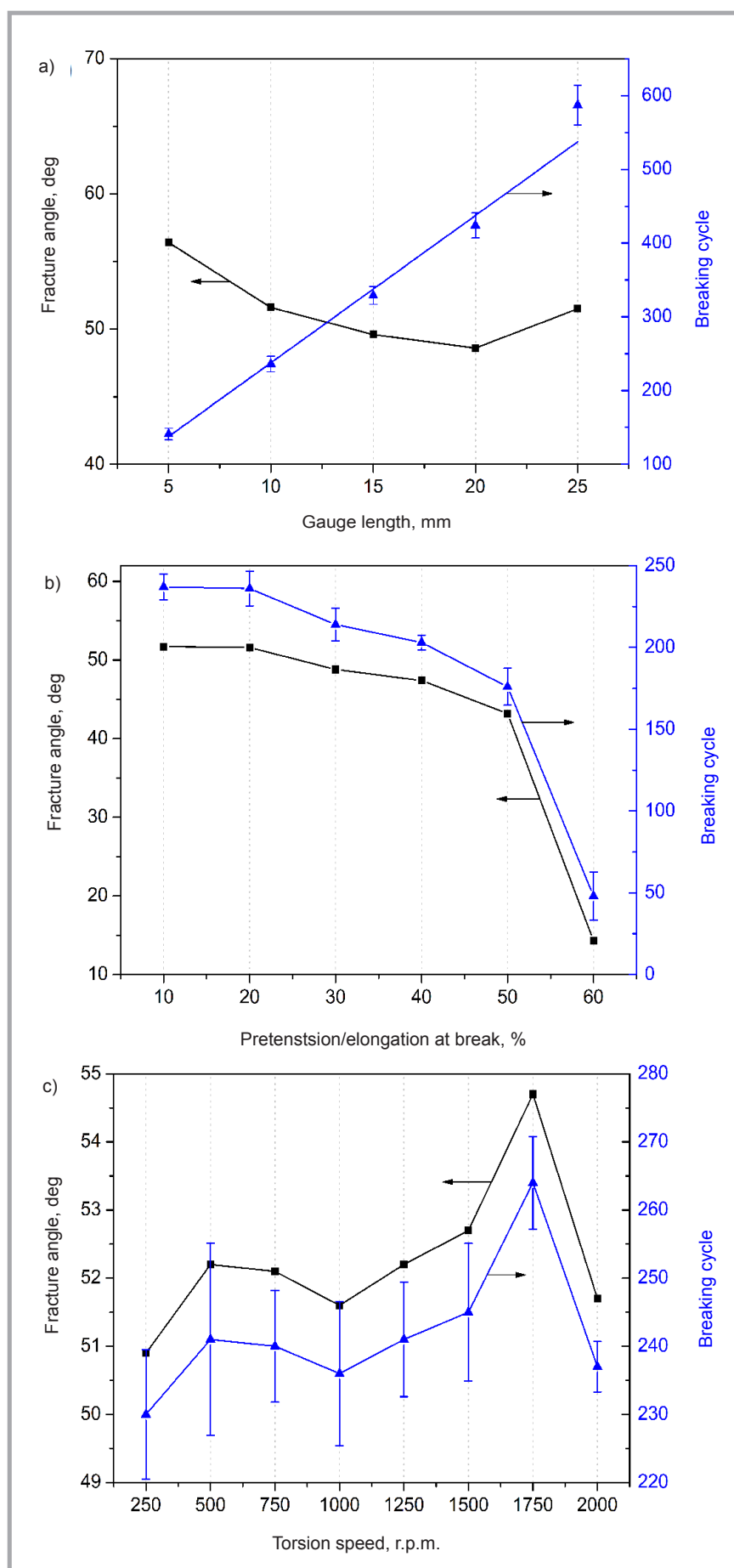


Figure 5. Effect of gauge length (a) pretension (b) and torsion speed (c) on the torsional fracture angle and breaking cycle of silk fibre.

Effect of the torsion speed on the unidirectional torsion performance

Figure 5.c shows the effect of the torsion speed on the torsion performance of single silk fibre. The general trend is that the fracture angle together with the breaking cycle increases with an increase in the torsion speed, as seen from Figure 5c. As the deformation of silk is a combination of irreversible and reversible viscose-elastic deformation, the irreversible deformation accumulates gradually, which takes time. As the torsion speed increases, the fibre is subject to quicker deformation in which irreversible deformation has insufficient time to accumulate. Thus the increase in torsion speed will dominate the reversible elastic deformation in the total deformation. The number of cycles needed to break the fibre will thus increase, and hence the fracture angle increases accordingly. However, the breaking cycle and fracture angle drops suddenly under extremely high torsion speed. In this situation, the fibre is subject to quick shearing deformation, which will lead to fracture in the structure of the fibre. It is evident that in practical application, silk fibre exhibits its poor performance when it is subjected to low speed torsion or extremely high speed torsion (e.g. 2000 r.p.m.). Proper parameter setting in spinning and careful usage of silk composites will prolong the service life of the products.

Conclusions

Unidirectional torsion was successfully exerted onto single silk fibre using a purpose-built single fibre mechanical property tester. Obvious spirals due to the twisting from torsion can be found on the surface of silk fibre from SEM photos. Silk fibre exhibits a ribbon-like profile after torsion, in which the two fibroin filaments are located side by side to form a helix. Fracture tends to occur at both ends of the silk fibre, where a larger number of twists can be observed. The crystallinity calculated from XRD spectra of silk fibre increases from 26.11 to 34.10% after torsion. This is due to the newly formed crystalline structure after torsion, as the macromolecular chains in the non-crystalline area are stretched and become closer and well-aligned to each other. The breaking stress and strain decrease slightly with an increase in the gauge length. It can also be seen that the breaking cycle increases linear-

ly with an increase in the gauge length. The actual torsional fracture angle decreases gradually with an increase in the gauge length, due to the possibility of the emergence of a weak point being higher when the gauge length increases. The torsional fracture angle together with the breaking cycle decreases gradually as the pretension increases from 10 to 50% of the tenacity. Too high a pretension, such as 60% of the tenacity, will lead to a drop in the fracture angle and breaking cycle. The fracture angle together with the breaking cycle increases with an increase in torsion speed.



References

1. Ude AU. Bombyx mori silk fibre and its composite: a review of contemporary developments. *Mater Design* 2014; 57: 298-305.
2. Shao Z and Vollrath F. Surprising strength of silkworm silk. *Nature* 2002; 418: 741.
3. Perez-Rigueiro J, Biancotto L, Corsini P, Marsano E, Elices M, Plaza GR and Guinea GV. Supramolecular organization of regenerated silkworm silk fibres. *Int J Biol Macromol* 2009; 44: 195-202.
4. Jelinski LW. Establishing the relationship between structure and mechanical function in silks. *Curr Opin Solid State Mater Sci* 1998; 3: 237-245.
5. Chen F, David P and Vollrath F. Silk cocoon (bombyx mori): multi-layer structure and mechanical properties. *Acta Biomater* 2012; 8: 2620-2627.
6. Arai T, Freddi G, Innocenti R and Tsukada M. Biodegradable of bombyx mori silk fibroin fibres and films. *J Appl Polym Sci* 2004; 91: 2383-2390.
7. Hearle JWS. *Atlas of fibre fracture and damage to textiles*. 2nd ed. Cambridge England: CRC press, 1998, p. 127.
8. Xu W. Research of repeated torsional fatigue property of textile fibre. *Cotton Text Technol* 1996; 6: 18-20.
9. Liu, X and Xu P. Study on torsion fatigue property of para-mid fibre. *Shanghai Text Sci Technol* 2004; 1: 8-9.
10. Feng H. Characterization of torsion fatigue of high-performance fibres. Master Thesis, Donghua University, China, 2005.

Received 31.08.2015 Reviewed 25.11.2015



Institute of Biopolymers and Chemical Fibres

FIBRES & TEXTILES in Eastern Europe reaches all corners of the world! It pays to advertise your products and services in our magazine! We'll gladly assist you in placing your ads.

FIBRES & TEXTILES in Eastern Europe

ul. Skłodowskiej-Curie 19/27
90-570 Łódź, Poland

Tel.: (48-42) 638-03-00
637-65-10

Fax: (48-42) 637-65-01

e-mail:

ibwch@ibwch.lodz.pl

infor@ibwch.lodz.pl

Internet:

<http://www.fibtex.lodz.pl>